Available online at www.sciencedirect.com

ScienceDirect

Procedia Computer Science 198 (2022) 148–155

Procedia Computer Science

www.elsevier.com/locate/procedia

The 11th International Conference on Current and Future Trends of Information and Communication Technologies in Healthcare (ICTH 2021)
November 1-4, 2021, Leuven, Belgium

A Systematic Evaluation of the XeThru X4 Ultra-Wideband Radar Behavior

Florentin Thullier[a,*], Alexandre Beaulieu[a], Julien Maître[a], Sébastien Gaboury[a], Kévin Bouchard[a]

[a] *Université du Québec à Chicoutimi, 555 Bd. de l'Université, Chicoutimi, Québec, G7H 2B1, Canada*

Abstract

Ultra-wide band radar systems have gained even more popularity as an emerging technology in health-related research and particularly in the context of ambient intelligence for activity recognition inside smart environments. Indeed, recent technological advances have facilitated their implementation on smaller SoC at lower cost. However, observed practical behaviors not always meet theoretical prediction. Therefore, this paper presents an empirical evaluation of Novelda XeThru X4-based IR-UWB radars behavior. To this end, several experiments were conducted to provide insightful analyses to consider while exploiting such recent technology. We believe that these assessments will benefit to academic researchers by guiding their implementation choices to design new robust activity recognition systems.

Keywords: UWB; Radar; XeThru; Activity Recognition; Ambient Intelligence

1. Introduction

Over the past decade, academic researchers multiplied their efforts providing solutions to cope with the world's growing aging population. Such aging of the population particularly affects Western societies, as healthcare and quality of life have improved substantially, leading to a direct influence on the global life expectancy [15]. For instance, the proportion of seniors aged over 65 in Canada has increased from 18.6% of the total population in 2003 to 22.3% in 2016 and is projected to reach up to more than 40% by 2063 according to forecasts [5]. As a result of such an increase in the number of elderly people, the ones suffering from a significant reduction of their autonomy, or even a total loss of it, will increase proportionally. Since such an autonomy decline may be correlated with neurodegenerative diseases

* Corresponding author. Tel.: +1-418-545-5011, ext. 2355.
E-mail address: florentin.thullier1@uqac.ca

10.1016/j.procs.2021.12.222

(*e.g.* Alzheimer disease), the demand for health-related services will also continue to increase tremendously. Indeed, impairments caused by these pathologies require a constant care and a rigorous assistance to achieve some or all of their activities of daily living (ADLs) [1]. Nowadays, in the context of a shortage of healthcare professionals, this assistance is mainly provided by family caregivers who must then assume the consequences of their involvement on a personal and emotional level as well as on a social and financial level [16].

Therefore, in order to overcome the complexity of providing a constant assistance for caregivers, the concept of ambient intelligence (AmI) emerged due to recent advances in information technology and microelectronics. AmI consists of enhancing a standard environment with technologies (*i.e.* sensors and actuators) to create a system having the ability to learn from its users' behaviors and to make decisions based on real-time information and historical data [17]. The main application of AmI is made inside smart homes, which represent an excellent means of assistance to support secure and semi-autonomous life for aging people [8]. In that sense, several smart home implementations [9, 6] have been built to be able to recognize ADLs also called human activity recognition (HAR). To achieve such a recognition, the literature identifies several techniques including three main approaches: video-based HAR [11], wearable sensor-based HAR [10] and non-wearable sensor-based HAR [7].

In the context of non-wearable sensor-based HAR, several research groups, including ours, have placed their efforts on the development of new methods that relies on the use of ultra-wide band (UWB) radio detection and ranging (radar) systems [3, 13, 14]. While these radars have been historically associated with large equipment for planes and boats detection, recent technological advances have facilitated their implementation on smaller systems on a chip (SoC) at lower cost enabling such a growing interest in the context of activity recognition inside smart environments. As a radio-frequency technology, UWB radars are theoretically well documented. Nevertheless, since it is a relatively emerging technology in health-related research, observed practical behaviors not always meet theoretical predictions. For instance, it has been reported that some influential factors such as moving people behind the wall where the radar is mounted may affect the expected behavior of UWB radars [3]. This leads us to state that developing robust prototypes for activity recognition remains a challenge for computer scientists. Hence, this paper suggests to study, in depth, the behavior of the most frequently employed UWB radar we found in the literature, namely, the Novelda XeThru X4 IR-UWB (impulse radio UWB) radar [3, 14, 2], from an empirical perspective. To do so, we designed a series of experiments that were conducted using three XeThru radars. The main purpose of this paper is to provide insightful analyses to consider while exploiting such recent technology.

2. Related Work

2.1. Ultra-Wideband Radars

The term ultra-wideband refers to a radio communication signal that has either a -10 dB bandwidth greater than 500 MHz or a -10 dB fractional bandwidth (the bandwidth divided by the band center frequency) greater than 20%. Such a large bandwidth enables UWB waves to propagate a large amount of data at a short distance. Since transmitters broadcast digital impulses, ultra-wideband are operating at very low power. Moreover, due to its high frequency pulse signals as opposed to amplitude, frequency or phase modulation UWB has been proposed to be more appropriate to an indoor usage due to a lower sensibility to the well-known multipath propagation problem [4].

In the context of IR-UWB monostatic radars such as the XeThru X4 chip, where transmitter and receiver are collocated, the transmitter first emits several UWB pulses (*i.e.* Pulse-Doppler). Once the pulse arrives to a focused object, the reflected pulse bounces back to the signal receiver, while the transmitted pulse passes through the object. It is thus possible to determine signals that have traveled to different distances through the measure of their time of arrival (TOA).

2.2. Activity Recognition Systems Using Ultra-Wideband Radars

Recently, UWB radars have been the subject of many promising works on various health-related fields of research including vital signs and sleep monitoring [18], indoor localization [4], fall detection [2] as well as activity recognition [14]. However, this section presents a review of proposed techniques mainly focused on activity recognition using UWB radar.

First of all, Jokanovic et al. [12] have proposed a system to achieve activity recognition exploiting raw data obtained from a single Ancortek SDR-RF 2500B module. Their system was evaluated through a dataset of four activities completed at 3.5 m away from the radar, in four different body orientations. The evaluation of the system demonstrates that certain domains are more favorable than others in recognizing specific activities using an UWB radar.

Next, Yang et al. [19] have also suggested the use of a single UWB radar (*i.e.* the PulsON 440). The effectiveness of the system has been evaluated by comparing the MOCAP dataset that includes emulated micro-Doppler data with their own dataset, both containing seven activities. The results obtained demonstrated the overall efficiency of exploiting the UWB technology to achieve the activity recognition process.

Finally, Bouchard et al. [3] and Maitre et al. [14] have proposed to achieve the activity recognition process inside smart homes using data from consumer-oriented IR-UWB radars. Indeed, the XeThru X4 chip embedded on these UWB radars has gained in popularity over the last two years due to their affordable price (MSRP fewer than 500 US dollars). Hence, a realistic dataset of 15 activities recorded with three XeThru X4M200 inside a smart home was used to evaluate both proposed systems. While accurate results were obtained by the authors, they also reported experiencing difficulties in generalizing their respective activity recognition models.

Through the review of these previously proposed works, we believe that employing a consumer-ready UWB radar such as the Novelda XeThru X4M200 requires a thorough study of its behavior to be appropriately deployed—particularly in the context of building robust activity recognition systems. Hence, this paper aims at providing an analysis of the X4 chip from an empirical perspective in order to help at better understanding the functioning of UWB radars. Moreover, it should benefit to academic researchers by guiding their implementation choices when designing a new system.

3. Hardware

The XeTrhu X4 chip is probably one of the first consumer-ready IR-UWB radars below 500 U.S. dollars currently available on the market. The two different SoCs available are the X4M300 and X4M200 sharing the same features except for the X4M200 that provides more advanced respiration and movement tracking software features. Moreover, the XeThru IR-UWB radar was designed to comply with UWB RF specifications of ETSI (European Telecommunications Standards Institute) in Europe, the FCC (Federal Communications Commission) in the USA and the ISED (Innovation, Science and Economic Development) in Canada. Indeed, it is possible for the lower pulse generator of the radar to transmit signals either on a low frequency within the 6.0 to 8.50 GHz band, or on a high frequency within the 7.50 and 10.20 GHz band under a low-emission level (*i.e.* $-41.30\, dBm/MHz$), reducing the radiation exposure. In that sense, long-term operations of these UWB radars inside a smart environment should not cause any health damage.

By default, these UWB radars allow data sampling at 17 frames per second. These frames are compiled in a buffer that is then processed by two parallel pulse-Doppler: the slow time exploits the last 20 seconds of data while the last 6 seconds are utilized by the fast time. Hence, the slow Doppler is used for respiration detection or a stationary/slow-moving person in the environment. However, we developed a custom data acquisition software to best suit the needs of our work. In that sense, the data sampling rate was changed to enable data acquisition up to 50 frames per second. Moreover, it allowed us to work directly with a buffer of frames that contains the raw data collected over a given period. These data are expressed as a radar scattering matrix, where each row represents the spatial samples from different ranges (*i.e.* bins or fast-time), and each column represents the frames recorded at different time intervals (*i.e.* slow-time). Finally, the maximum upper range of the detection zone we were able to reach using the custom software was 9.80 m, being a total of 184 single spatial samples or bins expressed in the form of complex numbers. This is about twice the default distance used for both the respiration and movement detection algorithms specified in the datasheet.

4. Data Collection Setup

In order to assess that the behavior of UWB XeTrhu radars is suitable to provide robust activity recognition systems inside smart environments, a comprehensive experimental protocol was designed. Thus, the data were collected by involving two people inside a controlled room of 250 m^2 free of any obstructive element (Figure 1). On the first hand, an observer was responsible for recording the dataset outside the field of operation of the radar. UWB data have been collected through many distance and height configurations (including empty space), each one of them was reproduced for three XeThru sensors (*i.e.* S_1, S_2, S_3). Hence, these radars have been successively plugged *via* USB to a laptop on which our custom acquisition software was executed. On the other hand, a subject was asked to either stand in front of the sensor or to move from side to side of the area of experimentation (13 m long by 4.60 m large) visually identified with colored tape. In both cases, the subject was requested to respect one of the six specific distances from the location of the radar (*i.e.* 0.30 m; 0.60 m; 1.20 m; 2.40 m; 4.80 m or 9.60 m). Moreover, since every XeTrhu X4M200 has been mounted on a stationary stand, several datasets were also collected from three distinct heights from the ground level (*i.e.* 0.45 m; 0.90 m or 1.35 m). All recordings were made for 22 seconds. Besides, we removed both the first and the last second were removed in order to avoid data inconsistencies. The data used in this paper was collected as part of a project reviewed and approved by the ethical board of our institution (#2019-220).

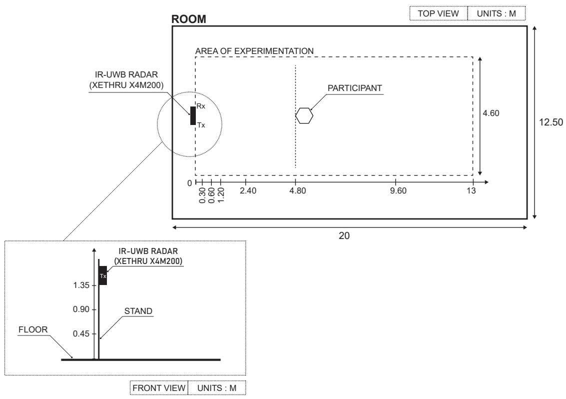

Fig. 1: Top and front views of the suggested experimental setup to complete the data collection.

5. Results & Discussion

The first step of our study was to determine the most significant bins to consider for the recognition of the six distances. Since we know that XeTrhu X4M200 was theoretically capable of operating in a range between 0.40 m and 9.80 m, where each recording frame contains 184 bins—a single bin thus corresponding to 0.053 m. In that sense, we were able to obtain the most relevant bin for each distance suggested by our experimental setup. However, since a single bin does not offer a sufficient degree of precision when identifying the distance of the subject from the radar, we judge that it was necessary to work with a set of bins of interest (BoI) instead. To do so, we assumed a variation of 0.30 m leading us to consider the three bins (*i.e.* 0.15 m) preceding and following the most significant one. Table 1 exposes the BoI for each distance used in the rest of the evaluations conducted.

Table 1: The bins of interest for each distance suggested by our experimental setup.

Distance	0.30 m	0.60 m	1.20 m	2.40 m	4.80 m	9.60 m
BoI	[3-9]	[8-14]	[20-26]	[42-48]	[87-93]	[177-183]

The first analysis we conducted in this work aimed at assessing whether the fluctuation of the data generated by each of our three radars appeared to follow a normal distribution. In that sense, a Shapiro–Wilk test of normality was performed for each radar on 20 s records corresponding to the data for an empty space (*i.e.* without the subject standing or moving in front of the radar) for each of the height configurations. A visual example of such recordings is provided by Figure 4a. In addition, Table 2 reports the proportion of bins by radar and height that are likely to be drawn from a normal distribution. The null hypothesis (H_0) was rejected when the p-value of a given bin was lower to an alpha level of $\alpha = 0.05$. Hence, according to the results obtained, it is possible to observe that the data quality and consistency of one X4M200 (*i.e.* S_2) significantly differ from the two others. This leads us to state that data produced by S_2 are more subject to noise than the ones obtained by the two other radars. While it is impossible for us to explain this finding with confidence, some potential avenues for further consideration may be explored. Indeed, it may be related to either imperfections or variability in the semiconductor manufacturing process or a misuse by our team compromising the integrity of this specific radar.

Table 2: The proportion of bins following a normal distribution for each radar and height configuration.

Sensor \ Height	$0.45\,m$	$0.90\,m$	$1.35\,m$
S_1	79 %	91 %	77 %
S_2	38 %	38 %	43 %
S_3	76 %	74 %	77 %

5.1. Distance From the Sensor

In order to evaluate the ability to accurately acquire distances with XeThru UWB radars, the standard deviation of each bin was computed for every distance on the data generated by one radar (*i.e.* S_1). Since the average of the bins was not sufficiently discriminative due to a large fluctuation of the values, the standard deviation was preferred as it remains more representative in evaluating the distance of the subject from the radar. Figure 2 illustrates a line chart of these variation measurements and demonstrates, for each distance, that a peak is noticeable in the range of BoI as defined previously.

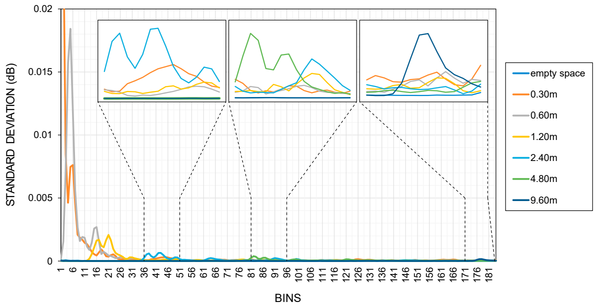

Fig. 2: Line chart of the standard deviation of each bin of the radar S_1 when mounted at $0.45\,m$, for each distance.

To confirm such an observation a two-tailed two-sample t-test between BoI and the remaining bins was performed for each distance and each height, where the degree of freedom is $df = (177\,bins + 9\,BoI) - 2$. Since these two sets of independent bins were not expected to have equivalent variance, a Welch's t-test was performed. Hence, the alternative hypothesis H_1 suggesting a significant difference between the two sets was accepted when the resulting p-values are lower than $\alpha = 0.05$. When such p-values were greater than α, no significant differences were determined, the null hypothesis H_0 was thus accepted. Table 3 reports obtained results and proves there is a significant difference for almost every configuration. As it is possible to observe both on the chart and through these results, when mounted at a $1.35\,m$ height, distances of $0.60\,m$ and $1.20\,m$ appears to be difficult to differentiate. This finding may be related to potential high reflections that may occur over short distances when the radar is installed this high, even in a controlled environment free of any obstacle. Thus, this suggests that the positioning of UWB radars should, in practice, not exceed a $0.90\,m$ height with a similar installation.

Table 3: Two-tailed two-sample Welch's t-tests $t(df)$ computed between bins of interest and remaining bins of radar S_1, where $df = 182$.

Distance \ Height	$0.45\,m$	$0.90\,m$	$1.35\,m$
$0.30\,m$	$t = 4.48.3, p = 0.003$	$t = 3.76, p = 0.008$	$t = 3.73, p = 0.009$
$0.60\,m$	$t = 4.38, p < 0.001$	$t = 2.92, p = 0.003$	$t = 1.69, p = 0.14$
$1.20\,m$	$t = 4.22, p = 0.005$	$t = 4.1, p = 0.001$	$t = -1.55, p = 0.14$
$2.40\,m$	$t = 3.65, p = 0.009$	$t = 4.36, p = 0.003$	$t = 2.53, p = 0.04$
$4.80\,m$	$t = 2.99, p = 0.02$	$t = 2.79, p = 0.03$	$t = 3.78, p = 0.005$
$9.60\,m$	$t = 4.4, p = 0.005$	$t = 3.93, p = 0.008$	$t = 16.7, p < 0.001$

5.1.1. Angle-of-Arrival

Another analysis that we considered important to provide was the impact on the capacity of the X4 chip to precisely recognize the distance when our subject was standing in front of one radar (*i.e.* S_1) mounted on the stand at $0.45\,m$ high and oriented at 45°. To do so, a standard two-tailed two-sample t-test was computed between the BoI for each orientation (*i.e.* 0° and 45°) at the same distance of $1.20\,m$ as an equal variance was expected in such experiment. According to the obtained result of $t(12) = 2.73$, $p = 0.018$, such a statistical test accepted the alternative hypothesis H_1. Hence, it remains possible to conclude that a relatively extreme orientation such as 45° has a significant influence on the accuracy of the identification of the distance. However, as shown by Figures 3 and 4d, only the amplitude of the peaks differ from one orientation to the other. Indeed, the peaks are observed in the same range of bins for both orientations at a distance of $1.20\,m$. This examination suggests that the radar orientation may not impact as significantly as the statistical analysis indicates. Nevertheless, we expect that the greater the orientation, the more the distance identification will be affected by undesirable reflections leading to a decrease in precision.

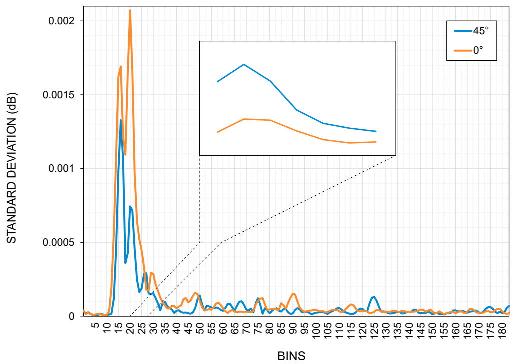

Fig. 3: Comparison of the standard deviation for both 0° and 45° orientations when the subject is standing at $1.20\,m$ from the radar S_1 when mounted at $0.45\,m$.

5.1.2. Movements

The analysis of the acquisition of movements was studied only by visualizing the spectrograms of the recorded UWB signals. An example is represented in Figure 4c. It refers to the recording of a linear movement from right to left made at $1.20\,m$ from the radar, which was mounted at a $0.45\,m$ height. The movement was repeated continuously throughout the $20\,s$ of data collection. Through this representation, it is possible to observe, between the bins of interest, that the signal generated by the movement may be characterized as a sine wave. This leads to believe that UWB technology and, more precisely, XeThru X4 SoC remain particularly well suited to recognize activities inside smart environments. The reviewed growing interest in this technology thus appears to be fully justified.

5.2. Height of the Sensor

Following evaluations regarding the distance of the X4M200, we placed our effort on providing an analysis of the impact of the radar height on its overall accuracy. To achieve this objective, we calculated the area under the curve (AUC) using the trapezoidal rule. It was computed through the absolute value of the arithmetic mean of the BoI for each distance and for each height of the radar. According to the results presented in Table 4, it is possible to state that the accuracy of identifying the farthest distances increases when the height of the UWB radar also grows. Indeed, the results show a significantly larger AUC up to $2.40\,m$ when the radar was placed at a $0.45\,m$ height. Then, a $0.90\,m$ height appears to be significantly more appropriate to precisely recognize distances from $2.40\,m$ to $4.80\,m$. Finally, for the distances around $9\,m$, no specific endorsement can be provided since the highest AUC obtained for a $1.35\,m$ height is not sufficiently distinct from the value of $0.45\,m$. This is not particularly surprising given that it refers to the maximum upper operating range of the X4 chip.

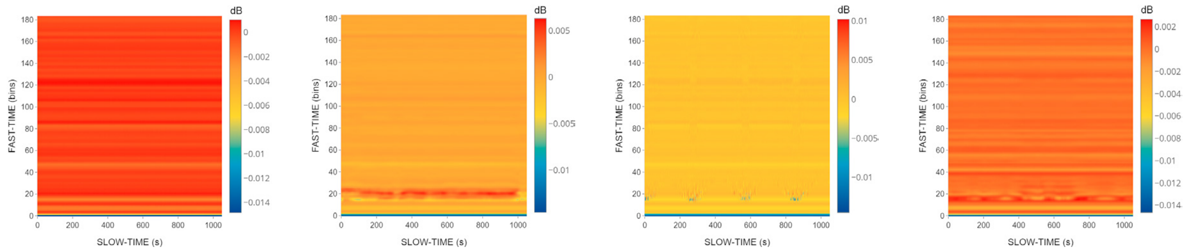

(a) radar orientation of 0° for an empty space

(b) radar orientation of 0° when the subject is stationary at a distance of 1.20 m

(c) radar orientation of 0° when the subject is moving at a distance of 1.20 m

(d) radar orientation of 45° when the subject is stationary at a distance of 1.20 m

Fig. 4: Spectrograms for radar S_1 when placed at 0.45 m high for four distinct configurations.

Table 4: Area under curve for each height configuration of the radar S_1 in relation with the absolute value of the arithmetic mean of the bins of interest for every distance.

Height \ *Distance*	0.30 m	0.60 m	1.20 m	2.40 m	4.80 m	9.60 m
0.45 m	0.0150	0.0083	0.017	0.0050	0.0012	0.0024
0.90 m	0.0059	0.0042	0.003	0.0024	0.0037	0.0013
1.35 m	0.0053	0.0054	0.001	0.0038	0.0010	0.0025

5.3. Inter-Sensors Variability

Finally, the last analysis provided in this work suggests to assess with details the possible variability existing in terms of precision between the three of our XeThru radars. To this end, we assumed that every radar had identical variances to compute a standard two-tailed two-sample t-test using the corresponding BoI of each distance for two distinct radars at a time. Table 5 presents the results obtained for the three 2-combinations possibles. Surprisingly, a majority of these statistical tests rejected the alternative hypothesis H_1 suggesting that, overall, there are no significant differences in precision between the three X4M200. The only significant variation observed remains between S_1 and S_3 at a distance of 9.60 m. Yet again, such a finding may be explained due to a distance close to the maximum capacity of the X4 chip. Therefore, regardless of the radar, distances around 9 m are more prone to be the most sensitive to minor changes, even in a controlled environment free of any obstacles.

Table 5: Two-tailed two-sample t-tests $t(df)$ computed for each 2-combinations of sensors at the same distance, where $df = 12$.

		2-combinations of sensors		
		$\{S_1, S_2\}$	$\{S_1, S_3\}$	$\{S_2, S_3\}$
Height	0.3 m	t = -0.07, p = 0.95	t = 0.04, p = 0.97	t = 0.12, p = 0.91
	0.6 m	t = -0.52, p = 0.6	t = -0.25, p = 0.8	t = -0.42, p = 0.68
	1.2 m	t = -0.75, p = 0.45	t = -1.32, p = 0.19	t = -0.79, p = 0.43
	2.4 m	t = -1.48, p = 0.14	t = -0.63, p = 0.53	t = 0.66, p = 0.51
	4.8 m	t = -0.57, p = 0.57	t = -1.45, p = 0.15	t = -0.97, p = 0.34
	9.6 m	t = -1.72, p = 0.09	t = -2.59, p = 0.01	t = -0.89, p = 0.38

6. Conclusion

Recently, with the commercialization of affordable UWB SoC, this technology has gained even more popularity as an emerging technology in health-related research and particularly in the context of activity recognition inside smart environments. However, some influential factors that may affect the nominal operation of such UWB radars were reported in the literature. Consequently, this paper suggested to study the behavior of the XeThru X4 UWB chips from an empirical perspective. In the first place, we found that the data quality and consistency of X4-based UWB radars may vary from one radar to another. Indeed, the data produced by one of our three radars were significantly more noisy, presumably due to imperfections or variability in the semiconductor manufacturing process. In addition, we observed that an elevated position for the radar may interfere with short distance recognition because of possible reflections that may occur. As regards the angle-of-arrival, we also showed that a decrease in precision is expected with a greater degree of orientation due to potential undesirable reflections. Finally, observations made on the recordings of the subject in movement lead us to verify that UWB technology is particularly well suited to recognize activities inside smart environments. The growing interest in this technology thus appears to be fully justified and very promising for future works.

Acknowledgements

The authors would like to thank the Ministère de l'Économie et de l'Innovation from the government of the province of Québec (Canada) for the grant that made this project possible as well as the Canadian Foundation for Innovation (CFI).

References

[1] Alzheimer's Association, 2021. 2021 Alzheimer's disease facts and figures. Alzheimer's & Dementia : the journal of the Alzheimer's Association 17, 327–406. doi:10.1002/alz.12328.
[2] Ayena, J.C., Chioukh, L., Otis, M.J.D., Deslandes, D., 2021. Risk of falling in a timed up and go test using an UWB radar and an instrumented insole. Sensors 21, 1–23. URL: https://www.mdpi.com/1424-8220/21/3/722, doi:10.3390/s21030722.
[3] Bouchard, K., Maitre, J., Bertuglia, C., Gaboury, S., 2020. Activity Recognition in Smart Homes using UWB Radars, in: Procedia Computer Science, Elsevier. pp. 10–17. doi:10.1016/j.procs.2020.03.004.
[4] Cemin, Z., Kuhn, M., Merkl, B., Fathy, A.E., Mahfouz, M., 2006. Accurate UWB indoor localization system utilizing time difference of arrival approach, in: Proceedings - 2006 IEEE Radio and Wireless Symposium, IEEE, San Diego, CA, USA. pp. 515–518. doi:10.1109/rws.2006.1615207.
[5] Chagnon, Jonathan; D'Aoust, Carol; Dion, Patrice; Galbraith, Nora; Sirag, Elham; Zhang, Y., 2019. Population Projections for Canada (2018 to 2068), Provinces and Territories (2018 to 2043). Technical Report. Statistics Canada.
[6] Cook, D.J., Crandall, A.S., Thomas, B.L., Krishnan, N.C., 2013. CASAS: A smart home in a box. Computer 46, 62–69. doi:10.1109/MC.2012.328.
[7] Fortin-Simard, D., Bilodeau, J.S., Bouchard, K., Gaboury, S., Bouchard, B., Bouzouane, A., 2015. Exploiting Passive RFID Technology for Activity Recognition in Smart Homes. IEEE Intelligent Systems 30, 7–15. doi:10.1109/MIS.2015.18.
[8] Giroux, S., Pigot, H., 2013. Smart Homes for People Suffering from Cognitive Disorders, in: Computer Science and Ambient Intelligence. Wiley, Hoboken, NJ USA, pp. 225–262. doi:10.1002/9781118580974.ch11.
[9] Helal, S., Mann, W., El-Zabadani, H., King, J., Kaddoura, Y., Jansen, E., 2005. The Gator tech smart house: A programmable pervasive space. Computer 38, 50–60. doi:10.1109/MC.2005.107.
[10] Hou, C., 2020. A study on IMU-based human activity recognition using deep learning and traditional machine learning, in: 2020 5th International Conference on Computer and Communication Systems, ICCCS 2020, IEEE. pp. 225–234. doi:10.1109/ICCCS49078.2020.9118506.
[11] Jalal, A., Mahmood, M., Hasan, A.S., 2019. Multi-features descriptors for Human Activity Tracking and Recognition in Indoor-Outdoor Environments, in: Proceedings of 2019 16th International Bhurban Conference on Applied Sciences and Technology, IBCAST 2019, IEEE. pp. 371–376. doi:10.1109/IBCAST.2019.8667145.
[12] Jokanovic, B., Amin, M., Erol, B., 2017. Multiple joint-variable domains recognition of human motion, in: 2017 IEEE Radar Conference, RadarConf 2017, IEEE, Seattle, WA, USA. pp. 0948–0952. doi:10.1109/RADAR.2017.7944340.
[13] Klavestad, S., Assres, G., Fagernes, S., Grønli, T.M., 2020. Monitoring Activities of Daily Living Using UWB Radar Technology: A Contactless Approach. IoT 1, 320–336. doi:10.3390/iot1020019.
[14] Maitre, J., Bouchard, K., Bertuglia, C., Gaboury, S., 2021. Recognizing activities of daily living from UWB radars and deep learning. Expert Systems with Applications 164. doi:10.1016/j.eswa.2020.113994.
[15] Organization, W.H., 2020. World health statistics 2020: monitoring health for the SDGs, sustainable development goals. Technical Report. World Health Organization.
[16] Paraponaris, A., Davin, B., Verger, P., 2012. Formal and informal care for disabled elderly living in the community: An appraisal of French care composition and costs. European Journal of Health Economics 13, 327–336. doi:10.1007/s10198-011-0305-3.
[17] Sadri, F., 2011. Ambient intelligence: A Survey. ACM Computing Surveys doi:10.1145/1978802.1978815.
[18] Shen, H., Xu, C., Yang, Y., Sun, L., Cai, Z., Bai, L., Clancy, E., Huang, X., 2018. Respiration and Heartbeat Rates Measurement Based on Autocorrelation Using IR-UWB Radar. IEEE Transactions on Circuits and Systems II: Express Briefs 65, 1470–1474. doi:10.1109/TCSII.2018.2860015.
[19] Yang, Y., Hou, C., Lang, Y., Guan, D., Huang, D., Xu, J., 2019. Open-set human activity recognition based on micro-Doppler signatures. Pattern Recognition 85, 60–69. doi:10.1016/j.patcog.2018.07.030.